EXPERIMENTAL STUDY OF DURABILITY OF REACTIVE POWDER CONCRETES

By N. Roux,[1] C. Andrade,[2] and M. A. Sanjuan[3]

ABSTRACT: The durability of reactive powder concretes (RPC) has been defined by measuring porosity, air permeability, water absorption, diffusion, and migration of chloride ions, accelerated carbonation, resistance to reinforcement corrosion, resistivity, and resistance to mechanical abrasion. Results were compared with the characteristics of a grade 30 MPa concrete with a low cement content and a grade 80 MPa very high performance concrete. The RPC displays excellent granular compactness, and its low water content helps reduce porosity. This results in an excellent resistance to the penetration of aggressive agents with respect to the reference concretes, and structures built with RPC are expected to significantly outlast those built with ordinary concrete.

INTRODUCTION

The resistance of concretes to aggressive agents is governed by the nature and severity of the environment as well as by the concrete mix design and constitution. Deterioration mechanisms, typically concrete carbonation and chloride attack, are principally caused by insufficient concrete impermeability and exaggerated porosity. The decrease of the water/cementitious ratio and addition of ultrafine particles contribute to improve the life of the concrete (Gjorv 1983; Nepper-Christensen et al. 1994).

High and very high strength concretes (60–120 MPa) have been used for structural elements for a long time (Vinches et al. 1993; Malier 1992). The mechanical properties are obtained by decreasing the water/cementitious ratio and often using superplasticizers and silica fume. This reduces the cement paste porosity and improves concrete durability.

Recently, compressive strengths of 200–800 MPa were obtained with reactive powder concretes (RPC) (Richard and Cheyrezy 1994). RPC is a family of concretes obtained by using four major principles:

- Improvement of the material homogeneity by removing all coarse aggregates
- Increase of the compactness by granular optimization and compaction
- Possible improvement of the microstructure by heat treatment
- Achievement of material ductility by the addition of steel fibers

The porosity of RPC is minimized by an optimized granular distribution with particles of different diameters ranging between fractions of a micron and 500 μm. The size of RPC micropores can be decreased by several orders of magnitude by an appropriate heat treatment after setting. The total RPC porosity is also modified by a pressurization of the sample during setting, which removes air bubbles and expels excess water from the cement paste.

Experimental results of tests on the resistance of RPC to aggressive agents are reported here.

[1]Prin. Engr., Bouygues-Challenger, Direction Scientifique Div. Constr., 1 E. Freyssinet, 78061 St. Quentin en Yvelines Cedex, France.

[2]Dir. and Res. Prof., Instituto de Ciencias de la Construction Eduardo Torroja, CSIC, Serrano Galvache, 28033 Madrid, Spain.

[3]Res. Asst., Instituto de Ciencias de la Construction Eduardo Torroja, CSIC, Serrano Galvache, 28033 Madrid, Spain.

Note. Discussion open until July 1, 1996. To extend the closing date one month, a written request must be filed with the ASCE Manager of Journals. The manuscript for this paper was submitted for review and possible publication on January 16, 1995. This paper is part of the ***Journal of Materials in Civil Engineering***, Vol. 8, No. 1, February, 1996. ©ASCE, ISSN 0899-1561/96/0001-0001–0006/$4.00 + $.50 per page. Paper No. 9960.

MATERIALS

The two concretes to be used as references in this study are representative of concretes with low cement contents on the one hand and very high strengths on the other. The mix design of the low cement content concrete (C30) that contains no admixtures yields a slump of 150 mm. The very high strength concrete (C80), with a high admixture content, contains 10% silica fume. Its compressive strength is high, and its low porosity assures good durability. The two reference concretes were obtained using the same cement of high characteristical strength, which explains their good mechanical properties.

The two reference concretes were mixed in a vertical-axis laboratory mixer having a capacity of 70 L. Half-crushed silicocalcareous sand and gravel were used. The gravel had a diameter between 4 and 14 mm. The characteristics of the concretes are provided in Table 1.

Two RPC were tested. The relative mix design of each was identical. The sole difference between the specimens produced was in the casting technique. The first one was table-vibrated in the laboratory (RPC200), whereas the second one was pressurized before and during setting (RPC200c) with a pressure of 60 MPa. The mix design of the RPC200 and RPC200c cement-based matrices are displayed in Table 2.

Some durability testing was conducted on material reinforced by metallic fibers at 2% of specimen volume, or the equivalent of 156 kg/m^3. The straight and cylindrical metallic fibers were 0.175 mm in diameter, 13 mm in length, and coated with a thin layer of brass. They were added to the mix at the end of the mixing process.

Experimental tests were performed on cylindrical specimens only. The C30 and C80 specimens measured 110 mm in diameter and 220 mm in height, while the RPC specimens were 70 mm by 140 mm. All specimens were cured 28 days in water at 20°C prior to undergoing various durability tests.

EXPERIMENTAL PROCEDURES AND RESULTS

The following tests provided experimental comparisons of the durability of C30, C80, and RPC concretes:

- Mercury porosimetry
- Air permeability
- Water absorption
- Diffusion and migration of chloride ions
- Carbonation rate
- Reinforcement corrosion rate
- Resistivity
- Resistance to abrasion

Mercury Porosimetry

Resistance to the penetration of aggressive agents in cement-based materials is primarily dictated by pore size, cu-

TABLE 1. Dry Mix Characteristics of C30 Low Cement Concrete and C80 Very High Performance Concrete

Mix characteristics (1)	C30 (2)	C80 (3)
Portland cement type V	300 kg/m³	450 kg/m³
Silica fume	—	45 kg/m³
Gravel/sand ratio	1.4	1.6
Water/cementitious (*W/C + SF*)	0.62	0.26
Superplasticizer (solid content)	—	5 kg/m³
Slump	150 mm	230 mm
f'_{c28}	35 MPa	90 MPa

TABLE 2. Dry Mix Design and Characteristics of RPC200 and RPC200c

Mix characteristics (1)	RPC200 (2)	RPC200c (3)
Portland cement type V	933 kg/m³	977 kg/m³
Silica fume	233 kg/m³	244 kg/m³
Sand (d_{sv} = 250 μm)	1,026 kg/m³	1,074 kg/m³
Superplasticizer (solid content)	13.8 kg/m³	14.5 kg/m³
Water	168 kg/m³	176 kg/m³
Water/cementitious (W/C + SF)	0.14	0.14
f'_{c28}	170 MPa	230 MPa

mulative porosity, and the degree of connection of these pores (connectivity). These parameters are determined, to a large extent, by the water/cementitious ratio. The use of water-reducing superplasticizers and optimization of the granular composition of the mix helps decrease the water content and thus the porosity of the concrete.

The distribution of pore diameters between 6 nm and 100 μm was measured with a Micromeritics pore size 9320 mercury porosimeter. The concrete samples (3–4 g) were extracted from the core of a specimen. They were heat-treated at 40°C for 24 hours, then held under a vacuum of 6 kPa for another 24 hours before being analyzed. The cumulative porosity of the four materials is compared in Fig. 1.

The cumulative porosity of the C80 concrete was brought down from 15% for the C30 to 10% by reducing the water/cementitious ratio from 0.62 to 0.26. This same principle, when applied to the RPC200 concrete, allowed reduction of the cumulative porosity measured between 6 nm and 100 μm to 1% for the sample that was not pressurized during setting and to 0.5% for the sample pressurized before and during setting (RPC200c). The absence of capillary pores could be observed along with a decrease in the microporosity threshold that defines the maximum size of the micropores. The influence of the casting technique and the microstructure modifications due to the posthardening heat treatment of RPC were already reported (Cheyrezy et al., in press, 1994).

Air Permeability

The permeability of cement-based matrices depends mainly on their system of pores, and also on their chemical and mineralogical composition. The extremely low porosity of C80 and RPC200 make the measurement of their water permeability difficult. The materials under study were, therefore, subjected solely to an air-permeability test.

The sensitivity of air-permeability measurement to variations in the material's moisture content necessitated the preconditioning of samples after they had been cured in water at 20°C for 28 days (Goto and Roy 1981). Two procedures for oven-drying were selected: (1) five days at 50°C; and (2) 30 days at 80°C (Ithuralde 1992).

Tests were conducted with an apparatus that respected the recommendations of CEMBUREAU (Kollek 1989). The measurement setup is illustrated in Fig. 2. The concrete sample extracted from the cylindrical specimen was 30 mm thick.

Air permeability K was calculated from the equation based on the Hagen-Poiseuille formula

$$K = \frac{2Q\mu Lp_a}{A(p^2 - p_a^2)} \quad (1)$$

with Q = air flow rate (in m³/s); μ = air viscosity [in Pa·s (1.9×10^{-5} Pa·s at 20°C)]; L = thickness of specimen (in m); A = cross-sectional area of specimen (in m²); p = source pressure (0.176 MPa); and p_a = atmospheric pressure (0.1 MPa).

The sensitivity threshold of the measurement apparatus is in the order of 10^{-18} m². Comparative results are shown in Table 3.

The air permeability of the RPC200 concrete is at least two orders of magnitude less than that of the C30 and C80 concretes. This feature, primarily due to the material's system of pores, is crucial in building resistance to the penetration of aggressive agents. This low permeability also presents opportunities for structures subjected to impermeability constraints (reservoirs, caissons, coatings, etc.)

Water Absorption

An excessive absorption of water by concrete can cause a certain number of structural disorders, notably the scaling of

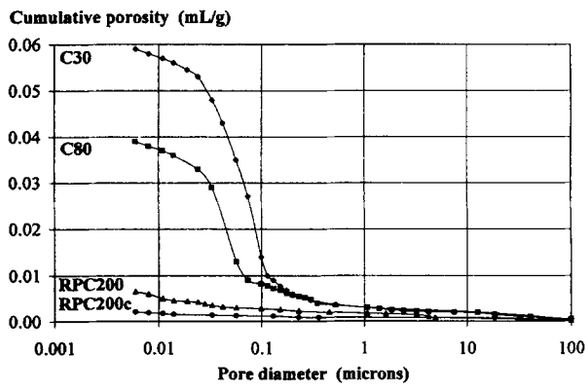

FIG. 1. Cumulative Porosity of RPC200 and RPC200c Compared to C30 and C80

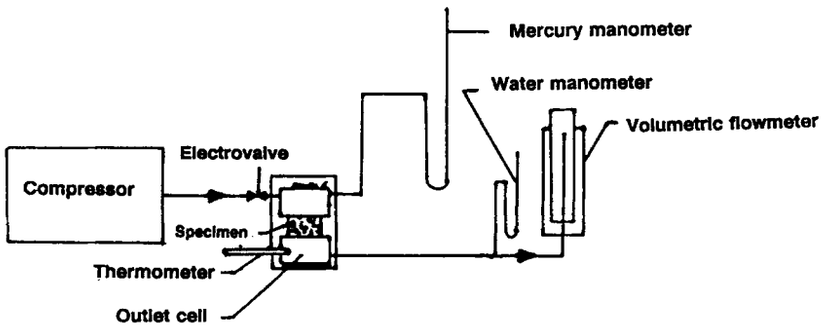

FIG. 2. Diagram of Apparatus Used to Measure Air-Permeability Coefficient

TABLE 3. Air Permeability of Nonpressurized RPC200 in Comparison with C30 and C80

Air permeability K, (m^2) (1)	Preconditioning of Samples	
	Five days at 50°C (2)	30 days at 80°C (3)
C30	30×10^{-18}	—
C80	0.3×10^{-18}	120×10^{-18}
RPC200	—	2.5×10^{-18}

FIG. 3. Measuring Water Absorption of Concrete

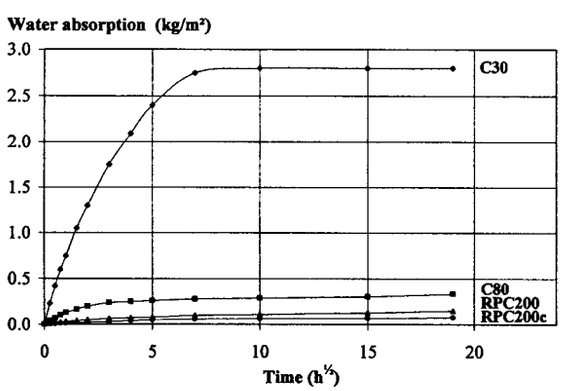

FIG. 4. Water Absorbed by RPC200 and RPC200c Compared to C30 and C80

the material through exposure to freezing/thawing and the corrosion of reinforcement from the penetration of chloride ions in tidal areas. The resistance of concrete to water penetration can be estimated by an experimental procedure (Fagerlund 1982). Defining the absorption kinetics and the quantity of water absorbed at equilibrium does provide an assessment of the absorption mechanisms as well as the diameter of the capillary pores.

Tests were conducted on 30-mm-thick cylindrical specimens that were 70 mm in diameter, cured 28 days in water at 20°C, and then stored in air at 20°C with a relative humidity of 50% until moisture equilibrium. The concrete slices were then placed on a water-saturated sponge and immersed in 5 mm of water. The testing tank is illustrated in Fig. 3. During the test period, the tank was covered by a plastic film to maintain a 100% relative humidity.

The specimens were weighed at specific time intervals. The surface of the slices was wiped with a slightly absorbent cloth prior to weighing. Results are expressed in terms of the quantity of water absorbed per unit surface area as a function of the square root of elapsed time. Fagerlund (1982) had determined that after a time t, an inflection point occurs on the curve that depicts the beginning of the stationary state. This inflection point is derived by extrapolating the points located at the beginning and the end of the test. It has thus been possible to calculate the values of two parameters: the resistance to water penetration and the coefficient of capillary absorption. The experimental curves are displayed in Fig. 4.

For the RPC200 concrete, no point of inflection in the experimental curve could be detected after 15 days of testing, and water absorption remained less than 0.2 kg/m^2. This very low level of absorption, coupled with the absence of an inflection point, is characteristic of a concrete with no capillary porosity, which has also been observed by mercury porosimetry. As a result, a very strong resistance to the penetration of aggressive agents is obtained.

Diffusion and Migration of Chloride Ions

The presence of chloride ions near metallic reinforcement is a major cause of corrosion. The passivating layer on the steel is attacked by chloride ions once their concentration exceeds a certain threshold level. Given the low porosity of RPC200, the diffusivity of chloride ions is initially assumed to be less than that for C30 concrete. Two types of tests have been used: a measure of simple diffusion and a measure of migration under steady-state chloride flow conditions based on differences in the electrical potential.

The test of simple diffusion by gravity consists of studying the concentration profile of chloride ions in a specimen sealed with an epoxy resin coating and equipped on top with a reservoir containing a 0.5 M NaCl solution. The chloride concentration was held constant throughout the one-year testing period. This method allowed evaluation of the apparent diffusion coefficient, D_a. The testing setup is highlighted in Fig. 5.

The interpretation of the concentration profile of chloride ions in the specimen of RPC200 does not yield conclusive findings on the penetration of ions during the testing period.

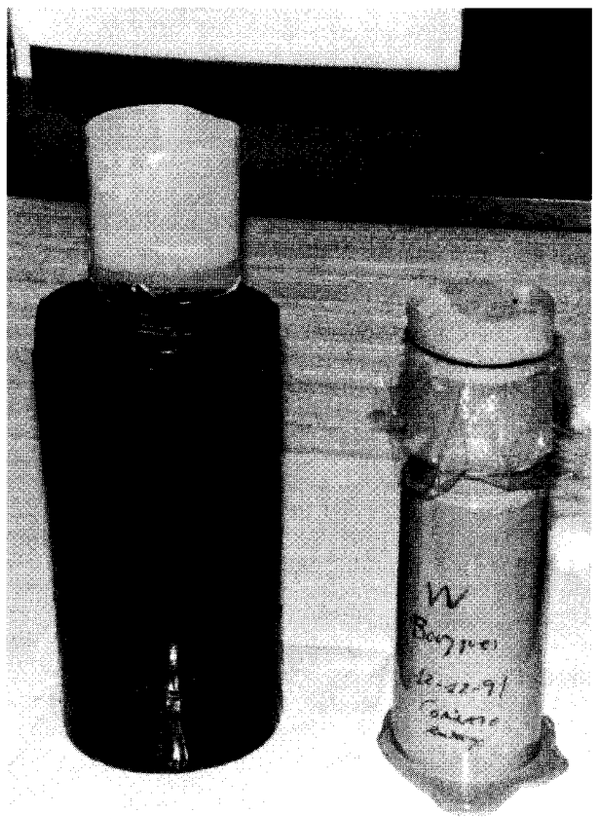

FIG. 5. Specimen during Testing of Simple Diffusion by Gravity

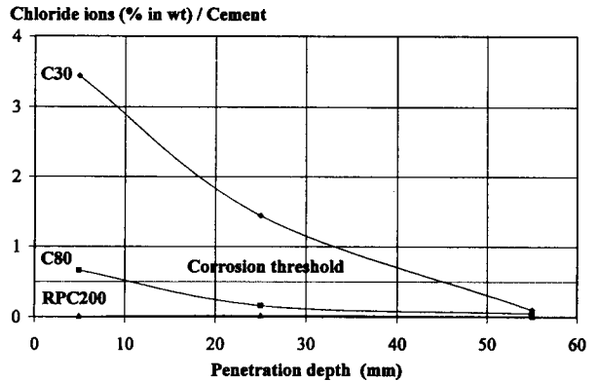

FIG. 6. Concentration Profile of Chloride Ions in C30, C80, and RPC200 Specimens for Use in Computation of Apparent Diffusion Coefficients

TABLE 4. Effective Diffusion Coefficient, D_{eff}, for C30, C80, and RPC200c

Diffusion coefficient (m^2/s) (1)	C30 (2)	C80 (3)	RPC200c (4)
D_{eff}	1.1×10^{-12}	0.6×10^{-12}	0.02×10^{-12}

The concentration varies between 0.01 and 0.03% of the concrete mass, which places it below the sensitivity threshold limit for the experimental method used. The concentration profiles measured on the three concretes C30, C80, and RPC200 are depicted in Fig. 6.

The migration measure of diffusion in steady-state chloride flow through differences in potential (12 V) requires the insertion of a 5-mm-thick concrete disc between two electrochemical cells: one cathodic, containing a 0.5 M NaCl solution, and the other anodic, containing distilled water (Andrade 1993). The chloride content of the two cells was observed over time from the point when steady-state migration had been reached. This procedure did allow for the determination of the effective diffusion coefficient, D_{eff}, computed using the Nernst-Plank equation. This computation did not take into consideration the chemical interactions between chloride ions and the material. Test results are summarized in Table 4.

The diffusion coefficient of RPC200c pressurized before and during setting is much lower than the coefficient associated with low cement concrete.

Carbonation Rate

The resistance of concrete to carbon dioxide was measured by a natural carbonation test and two accelerated carbonation tests. The curing conditions selected were: (1) Exposure to ambient conditions [0.03% CO_2/50% relative humidity (RH)] for 18 months; (2) accelerated test at 60% relative humidity and 5% CO_2 for 42 days; and (3) accelerated test as described, followed by 90 days at 100% CO_2. The carbonation of concrete is monitored by a phenolphthalein color indicator. Although the carbonation coefficient of the C30 concrete reached 50 mm/$yr^{0.5}$, after the accelerated treatment at 100% CO_2, no carbonation could be detected on RPC200.

Reinforcement Corrosion Rate

The corrosion of metallic reinforcement in concrete results from electrochemical reactions, with the interstitial water acting as the electrolyte. The reinforcement can behave either as the cathode or the anode, and the steel deterioration results from chemical reactions. Initially, the cement-based matrix ensures the protection of the steel by promoting the formation of a passivating layer. The drop in pH caused by the carbonation of the matrix or the presence of chloride ions can trigger the corrosion process. The electrolyte plays a pivotal role in assuming three distinct functions: (1) The diffusion of aggressive agents, mainly CO_2 and the chloride ions; (2) the passage of electrical current of an ionic nature; and (3) the passage of products formed during the corrosion of steel.

The corrosion of reinforcement embedded in the different concretes was analyzed through electrochemical measurements. Two tests were carried out: the polarization resistance test and the electrochemical impedance spectroscopy. The cylindrical specimens studied were cast with two 3-mm-diameter steel rods embedded in the concrete. The concrete-reinforcement interface was isolated by an adhesive ribbon. The length of steel in contact with the concrete was 30 mm.

The first method involves application of a potentiodynamic sweep from −10 to +10 mV at the corrosion potential, E_{corr}. The determination of the intensity, I, enables calculation of the polarization resistance, R_p, without disturbing the corrosion reactions at the metal-electrode interface (Andrade et al. 1986). The corrosion intensity, I_{corr}, is calculated by Stern's (Stern and Weisert 1959) equation: $I_{corr} = B/R_p$, with the coefficient B assumed to have a value of 26 mV for corroding steel and 52 mV for passivated steel. Monitoring of the corrosion intensity I_{corr} over time allows estimation of the loss of mass per unit of time and surface. A reinforcement corrosion rate, v_{corr}, can thereby be defined in terms of micrometers per year. It has commonly been recognized that no corrosion risk in concrete exists for values less than 1 μm/year.

In addition to the test of polarization resistance, the electrochemical impedance spectroscopy has confirmed, through a dynamic method, the results obtained earlier. The measurement principle is identical to the aforementioned, except that the potentiodynamic shift is applied by a variable frequency. The use of frequencies varying between 0.1 mHz and 100 kHz with amplitudes of 8 mV provides information on the kinetics of corrosion reactions. Further details on the experimental pro-

TABLE 5. Results of Corrosion-Resistance Tests

Impedance test (1)	Corrosion threshold (2)	C30 (3)	C80 (4)	RPC200 (5)
E_{corr} (in mV)	>−200	−0.82	+0.28	+0.90
R_Ω (in kΩ·cm^2)	>500	0.37	12	3,022
C_{HF} (in pF/cm^2)	—	10,793	145	14
v_{corr} (in μm/yr)	<1	1.2	0.25	<0.01

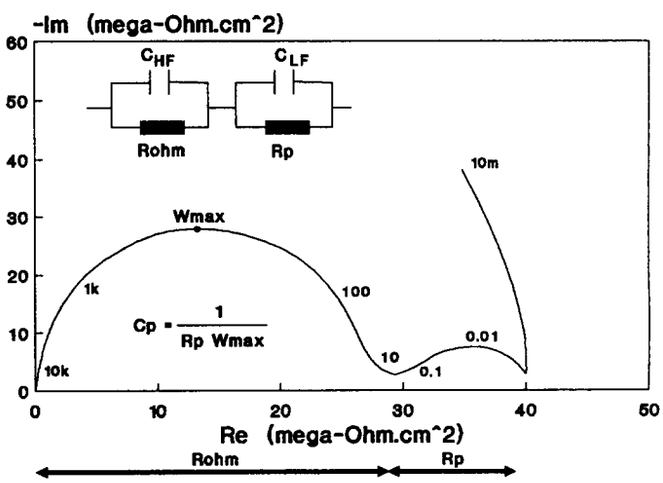

FIG. 7. Nyquist Diagram for RPC200

TABLE 6. Resistivity of C30, C80, and RPC200

Resistivity (kΩ·cm) (1)	C30 (2)	C80 (3)	RPC200 (4)
ρ	16	96	1.13×10^3

cedure used, the testing apparatus, and the interpretation of measurements are given elsewhere (Andrade et al. 1986; Xu et al. 1993).

All test specimens were cured at 25°C and 100% relative humidity for 230 days.

The data computed from the resulting Bode and Nyquist diagrams are presented in Table 5. The Nyquist diagram of the RPC200 concrete is illustrated in Fig. 7. The interpretation of these diagrams requires the introduction of a model describing the ohmic resistance of the electrolyte, R_Ω, the faradic impedance, Z_F, and two capacitances C_{HF} and C_{LF}. With this model, the time constants of the reactions under study can be interpreted.

A very high ohmic resistance is observed in the case of RPC200, in comparison with that of C30 or C80. This feature helps hinder the passage of electrical current of an ionic nature, which further slows down all corrosion reactions. The values of capacitance indicate that the dielectric properties of RPC200 are much superior to those of C30 and C80. The calculation of the corrosion rate yields an extremely low value that justifies disregarding any concern about the corrosive activity.

Visual inspection of the specimens and of the steel reinforcement at the end of testing did not indicate the presence of corrosion.

Resistivity

The resistivity, ρ, of the tested concretes was measured with the help of two electrodes placed on the upper and lower faces of a cylindrical specimen. Resistivity is obtained from Ohm's law

$$\rho = R_\Omega \cdot A/l \tag{2}$$

where R_Ω = electrical resistance of the concrete (in kΩ); A = cross-sectional area of the specimen (in cm^2); and l = distance between electrodes (in cm).

Conductivity measurements were performed on specimens that were cured in 20°C water for 28 days, then maintained 30 days at 92% relative humidity and an additional 30 days at 100% relative humidity. The results are listed in Table 6. It was verified that the electrical resistance measured by the resistivity method was identical to that measured by the electrochemical impedance methods or by the more classical conductivity method.

The presence of metallic fibers causes the material's resistivity to fall from 1.13×10^3 kΩ·cm to 137 kΩ·cm. The extremely high resistivity of RPC200's cement-based matrix leads to an efficient protection of the metallic fibers and the steel embedded in the material.

The sensitivity of RPC200's cement-based matrix to variations in humidity is low. Reducing humidity in the cement-based matrix by heat treatment (six days at 50°C) increases the resistivity from 1.13×10^3 to 1.20×10^3 kΩ·cm.

Resistance to Abrasion

The resistance of RPC200 to mechanical abrasion was confirmed by the Compagnie Nationale du Rhône (CNR) test. The material immersed in water was subjected to a silica sand blast jet at a pressure of 250 kPa oriented at 45°. Following a specific time interval, the volume of the specimen's imprint was measured. This volume was then compared with the one obtained on a reference specimen of glass in order to determine the abrasion coefficient I.

$$I = \frac{V}{V_0} \tag{3}$$

with V = volume of the imprint on the material; and V_0 = volume of the imprint on the reference glass.

The test apparatus is illustrated in Fig. 8, and abrasion coefficients for different concretes are presented in Table 7.

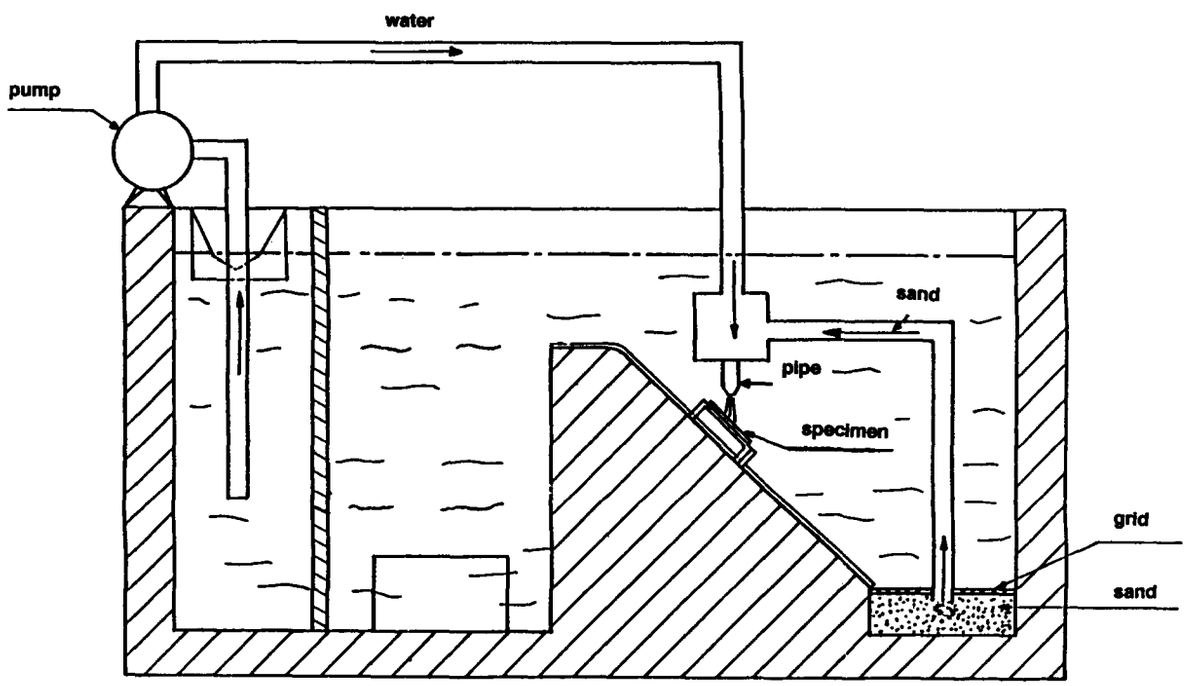

FIG. 8. Apparatus Used to Measure Abrasion Coefficient, Following CNR Procedure

TABLE 7. Abrasion Coefficients Measured with CNR Testing Procedure; Coefficient is Equal to One for Reference Material, Glass

Abrasion coefficient (1)	C30 (2)	C80 (3)	RPC200 (4)
Coefficient *I*	4.0	2.8	1.3

RPC200's resistance to abrasion can be compared to that of a mortar cast with corundum aggregate with an abrasion coefficient *I* of the order of 1.2 (Dauriac, unpublished report, 1994).

CONCLUSION

The fundamental experimental results obtained on RPC200 were the absence of pores with diameters exceeding 15 nm; an air permeability coefficient of 2.5×10^{-18} m^2, following exposure to severe drying conditions (30 days at 80°C); extremely low water absorption; an effective diffusion coefficient 50 times less than that of low cement concrete; no carbonation after exposure to 5% CO_2 for 42 days (60% relative humidity) and to 100% CO_2 for 90 days; a reinforcement corrosion rate lower than 0.01 μm/yr (corrosion threshold = 1 μm/yr); a resistivity of RPC200's cement-based matrix 70 times higher than that of C30 concrete, and an abrasion coefficient comparable to that of a mortar cast with a corundum aggregate.

The extremely high resistance of RPC200 and RPC200c concrete to the penetration of aggressive agents corresponds to excellent durability characteristics, thereby yielding a significant increase in the life expectancy of structures built with reactive powder concretes.

APPENDIX. REFERENCES

Andrade, C. (1993). "Calculation of chloride diffusion coefficients in concrete from ionic migration measurements." *Cement and Concrete Res.*, 23(3), 724–742.

Andrade, A., Castello, V., Alonso, C., and Gonzalez, J. A. (1986). "The determination of the corrosion rate of steel embedded in concrete by the polarization resistance and AC impedance methods." *STP906*, V. Chaker, ed., ASTM, Philadelphia, Pa., 43–63.

Fagerlund, G. (1982). "On the capillarity of concrete." *Nordic Concrete Res.*, Vol. 1, 6.1–6.20.

Gjorv, O. E. (1983). "Durability of concrete containing condensed silica fume." *Fly ash, silica fume, slag & other mineral by-products in concrete; Publ. SP-79*, Am. Concrete Inst. (ACI), Detroit, Mich., 695–708.

Goto, S., and Roy, D. M. (1981). "The effect of w/c ratio and curing temperature on the permeability of hardened cement paste." *Cement and Concrete Res.*, 11(4), 575–580.

Ithuralde, G. (1992). "Permeability: the owner's viewpoint." *High performance concrete*, Y. Malier, ed., E & FN Spon, London, England, 276–294.

Kollek, J. (1989). "Mesure de la perméabilité du béton à l'oxygène par la méthode Cembureau, Recommendation." *Ciments, bétons, plâtres, chaux*, SEPTIMA, Paris, France, No. 778, 169–173 (in French).

Malier, Y. (ed.) (1992). High performance concrete, E & FN Spon, London, England.

Nepper-Christensen, P., Kristensen, B. W., and Rasmussen, T. H. (1994). "Long-term durability of special high strength concretes." ACISP 145-9, Detroit, Mich., 173–190.

Richard, P., and Cheyrezy, M. (1994). "Reactive powder concretes with high ductility and 200–800 MPa compressive strength." *Proc., ACI Spring Convention; SP144-24 (91-AB).*

Stern, M., and Weisert, E. D. (1959). *Proc., 59*, ASTM, Philadelphia, Pa., 1280–1291.

Vinches, M., Leguet, J. L., and Dugat, J. (1993). "The amphitheatre of Ales School of Mines: an experimental building for high performance concretes." *Proc., High strength concrete*, 599–606.

Xu, Z., Gu, P., Xie, P., and Beaudouin, J. J. (1993). "Application of AC impedance techniques in studies of porous cementitious materials." *Cement and Concrete Res.*, 23(3), 531–540.